



INTEGRAL

Announcement of Opportunity for Observing Proposals (AO-3)

JEM-X Observer's Manual

Written by: Astrid Orr
Integral Science Operations, ESTEC

based upon inputs from the JEM-X team
DSRI, Copenhagen
(PI: N. Lund)

13 September 2004
Issue 3

Ref. nr. INT-SOC-DOC-023

This page was intentionally left blank

Table of Contents

I.	Introduction	5
II.	Description of the instrument	7
1.	The overall design and status	7
2.	The detector	8
3.	The coded mask	9
III.	Instrument operations	11
1.	Telemetry formats and their use	11
2.	The grey-filter mechanism	11
3.	Detailed overview of the telemetry formats	12
3.1	Combining primary and secondary telemetry formats	14
3.2	Ranges of usefulness of telemetry formats	14
IV.	Performance of the instrument	16
1.	Background	16
2.	Timing stability and resolution	16
3.	Imaging: resolution and detection limits.	16
4.	Detector energy resolution	18
5.	Sensitivity (continuum and lines)	19
V.	Observation “cook book”	23
1.	Considerations of the use of the instrument	23
2.	Loss of JEM-X sensitivity due to dithering	23
3.	How to estimate observing times	24
3.1	Continuum emission	24
3.2	Line emission	26
4.	Practical examples	26
4.1	Example #1: spectroscopy and continuum studies	26
4.2	Example #2: broad band variability	27
4.3	Example #3: broad band variability and dithering	27
4.4	Example #4: line detection	28
4.5	Example #5: in-orbit count rates for the Crab and the background	28

This page was intentionally left blank

I. Introduction

The Joint European Monitor for X-rays (JEM-X) on-board INTEGRAL fulfils three roles:

- 1) It provides complementary data at lower energies for the studies of the gamma-ray sources observed by the two main instruments, IBIS and SPI. Normally any gamma-ray source bright enough to be detected by the main instruments will also be bright enough to be rapidly identified with JEM-X. Note, however, that the field of view of JEM-X is significantly smaller than those of IBIS and SPI. Flux changes or spectral variability at the lower energies may provide important elements for the interpretation of the gamma-ray data. In addition, JEM-X has a higher spatial resolution than the γ -ray instruments. This helps with the identification of sources in crowded fields.
- 2) During the recurrent scans along the galactic plane JEM-X provides rapid alerts for the emergence of new transients or unusual activity in known sources. These sources may be unobservable by the other instruments on INTEGRAL.
- 3) Finally, JEM-X can deliver independent scientific results concerning sources with soft spectra, serendipitously detected in the field of view (FOV) during the normal observations.

JEM-X operates simultaneously with the main gamma-ray instruments IBIS and SPI. It is based on the same principle as the two gamma-ray instruments on INTEGRAL: sky imaging using a coded aperture mask. The performance of JEM-X is summarised in Table 1.

Table 1: parameters and performance of the JEM-X1 unit

Parameter	In-orbit value
Active mask diameter	535 mm
Active detector diameter	250 mm
Distance from mask to detector entrance window	3401 mm
Energy range	3-35 keV
Energy resolution (FWHM)	$\Delta E/E = 0.40 \times [(1/E \text{ keV}) + (1/120 \text{ keV})]^{1/2}$
Angular resolution (FWHM)	3'
Field of view (diameter)	4.8° Fully illuminated 7.5° Half response ^a 13.2° Zero response
Relative point source location error	1' (90% confidence radius for a 15 σ isolated source)
Continuum sensitivity for a single JEM-X unit (isolated source on-axis)	$1.2 \times 10^{-4} \text{ ph cm}^{-2} \text{ s}^{-1} \text{ keV}^{-1}$ @ 6 keV $1.0 \times 10^{-4} \text{ ph cm}^{-2} \text{ s}^{-1} \text{ keV}^{-1}$ @ 30 keV for a 3 σ cont. detection in 10 ⁵ s, dE = 0.5E
Narrow line sensitivity for a single JEM-X unit (isolated source on-axis)	$1.6 \times 10^{-4} \text{ ph cm}^{-2} \text{ s}^{-1}$ @ 6 keV $1.3 \times 10^{-4} \text{ ph cm}^{-2} \text{ s}^{-1}$ @ 20 keV for a 3 σ line detection in a 10 ⁵ s observation
Timing resolution	122 μs (relative timing) $\approx 1 \text{ ms}$ (absolute timing)

a. At this angle the sensitivity is reduced by a factor 2 relative to the on-axis sensitivity. In practice, the transmission of the collimator beyond an off-axis angle of 5° is so low that only the very brightest sources can be observed at larger angles

II. Description of the instrument

1. The overall design and status

JEM-X consists of two identical coded-aperture mask telescopes co-aligned with the other instruments on INTEGRAL. In the current configuration the JEM-X “1” unit is operating while JEM-X “2” is dormant. The photon detection system of JEM-X consists of high-pressure imaging Microstrip Gas Chambers located at a distance of 3.4 m from each coded mask. Figure 1 shows a schematic diagram of one JEM-X unit. A single JEM-X unit comprises 3 major subsystems: the detector, the associated electronics and the coded mask.

At the end of the Instrument Performance Verification phase, it was decided to operate only one JEM-X unit at a time. The switch-off of one of the units was decided after a gradual loss in sensitivity had been observed in both JEM-X units, due to the erosion of the microstrip anodes inside the detector. By lowering the operating voltage, and thereby the gain of the detectors, the anode damage rate has now been reduced to a level where the survival rate of the detectors seems to be assured for the extended mission phase. If in the future both units are to be switched on together again, the total sensitivity will increase by approximately a factor $\sqrt{2}$, however at the time of writing of this document such a change is not being considered.

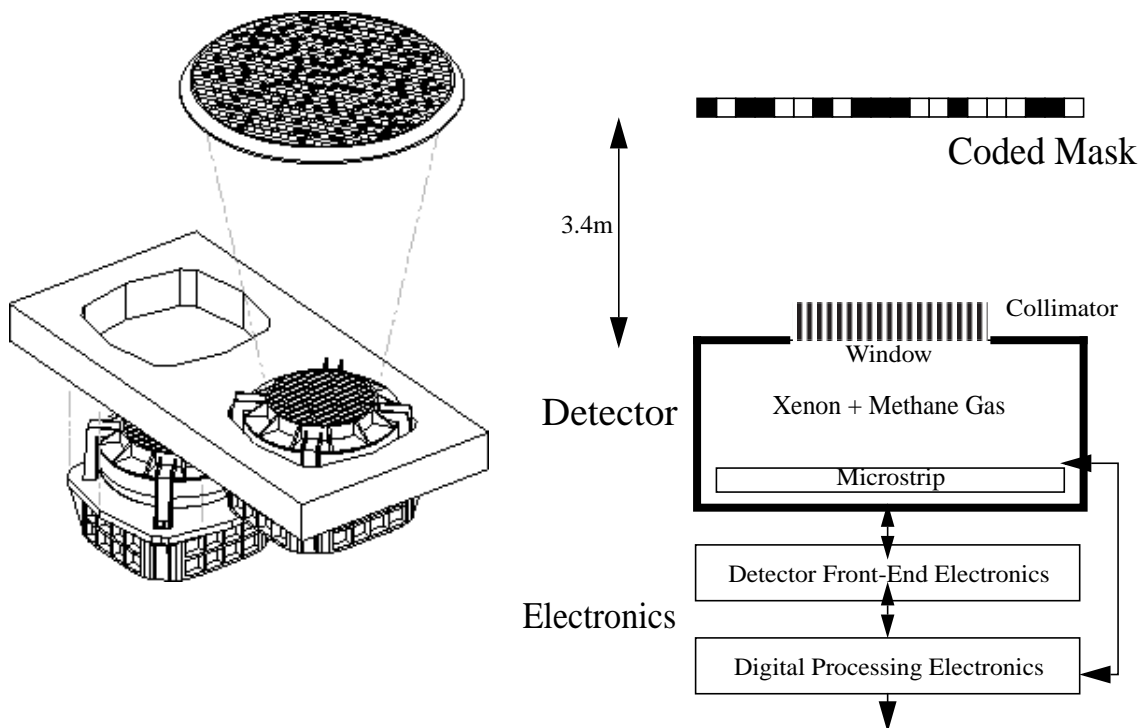


Figure 1. Left: overall design of JEM-X, showing the two units, with only one of the two coded masks. Right: functional diagram of one unit

2. The detector

The JEM-X detector is a microstrip gas chamber with a sensitive geometric area of $\sim 500 \text{ cm}^2$ per unit. The gas filling is a mixture of xenon (90%) and methane (10%) at 1.5 bar pressure. The incoming photons are absorbed in the xenon gas by photo-electric absorption and the resulting ionisation cloud is then amplified in an “avalanche” of ionisations by the strong electric field near the microstrip anodes. Significant electric charge is picked up on the strip as an electric impulse. The position of the electron avalanche in the direction perpendicular to the strip pattern is measured from the centroid of the avalanche charge. The orthogonal coordinate of an event is obtained from a set of electrodes deposited on the rear surface.

The X-ray window of the detector is composed of a thin (250 μm) beryllium foil which is impermeable to the detector gas but allows a good transmission of low-energy X-rays.

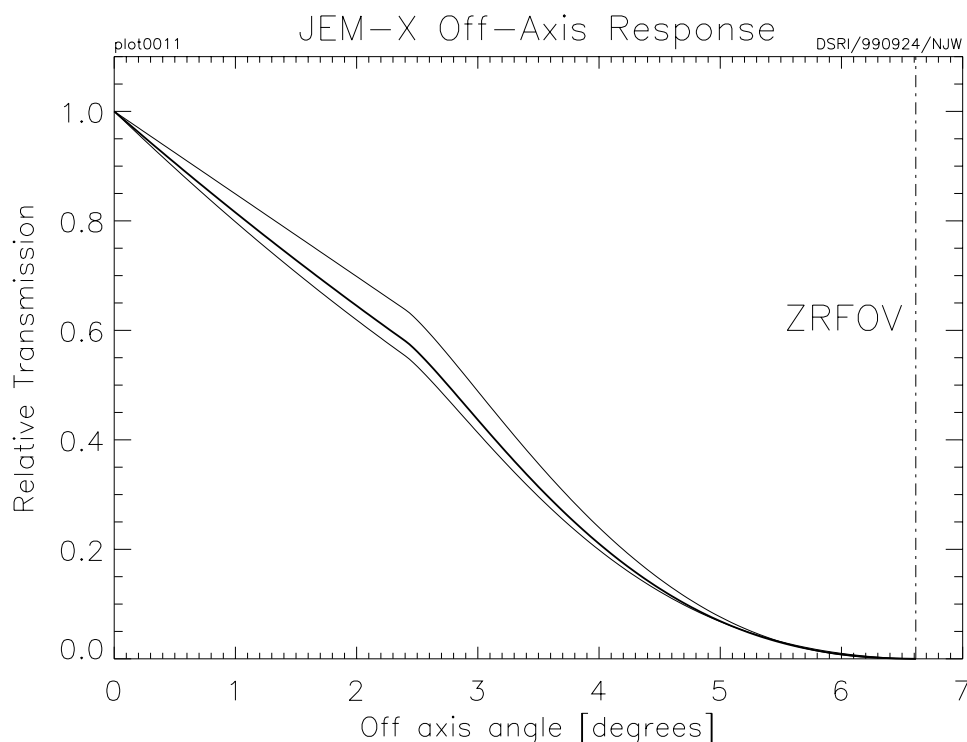


Figure 2. Off axis response of JEM-X below 50 keV. The middle curve shows the average transmission through the collimator including all azimuth angles. The square pattern of the collimator introduces an azimuthal dependence of the throughput with a minimum and a maximum as indicated by the two outer curves. (Response=0 at ZRFOV)

A collimator structure with square-shaped cells is placed on top of the detector entrance window. It gives support to the window against the internal pressure and, at the same time, limits and defines the field of view of the detector. It has an 85% on-axis transparency. The collimator is important for reducing the count rate caused by the cosmic diffuse X-ray background. However, the presence of the collimator also means that sources near the edge of the field of view will be attenuated with respect to on-axis sources (see Fig. 2). The materials for the collimator (molybde-

num, copper, aluminium) have been selected in order to minimise the detector background caused by K fluorescence.

Four radioactive sources are embedded in each detector collimator in order to calibrate the energy response of the JEM-X detectors in orbit. Each source illuminates a well defined spot on the microstrip plate. The gain of the detector gas is monitored continuously with the help of these sources. Figure 3 shows the collimator layout and the locations of the calibration sources.

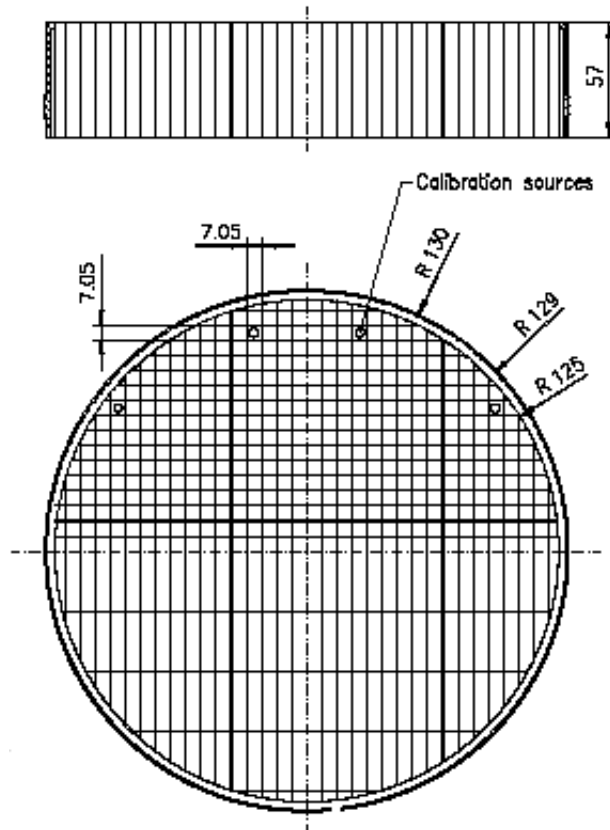


Figure 3. Collimator layout. In this diagram the 4 calibration sources are situated on the upper side. The dimensions are in mm, i.e. collimator length = 57 mm, radius = 130 mm

3. The coded mask

The mask is based on a Hexagonal Uniformly Redundant Array (HURA). For JEM-X a pattern composed of 22501 elements with only 25% open area has been chosen. The 25% transparency mask actually achieves better sensitivity than a 50% mask, particularly in complex fields with many sources, or in fields where weak sources should be studied in the presence of a strong source. A mask with lower transparency also has the advantage of reducing the number of events to be transmitted, while at the same time increasing the information content of the remaining

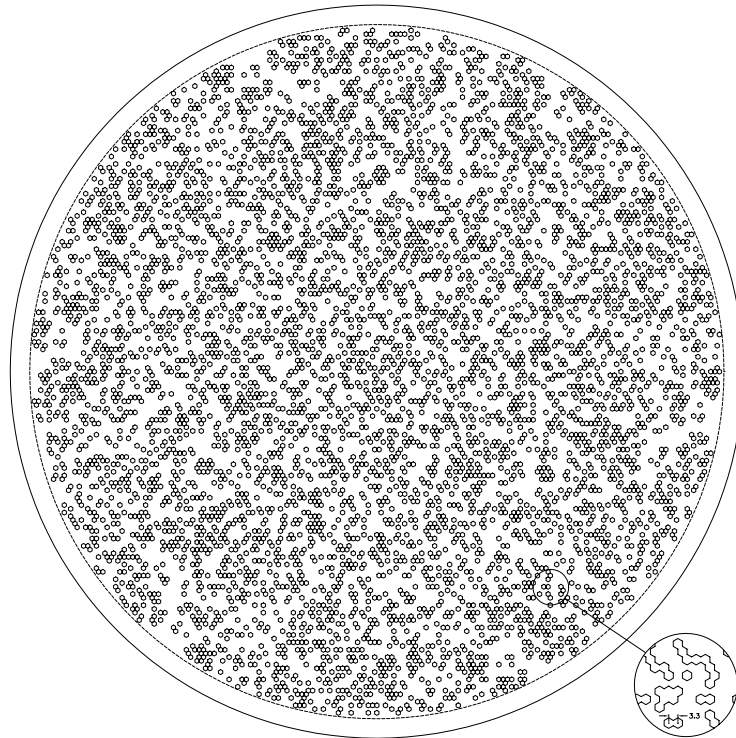


Figure 4. Illustration of the JEM-X coded mask pattern layout without the mechanical interface. The diameter of the coded mask is 535 mm. The mask has a transparency of 25%

events. Considering the telemetry allocation to JEM-X, this means an improved overall performance for the instrument, particularly for observations in the plane of the Galaxy.

The JEM-X imaging is affected by some (limited) coding noise, but does not suffer from “ghost” images because the pattern of the mask only repeats itself near the edges of the mask.

The mask height above the detector (~ 3.4 m) and the hexagonal mask element dimension (3.3 mm centre-to-centre) define together the angular resolution of the instrument, in this case $3'$. Figure 4 illustrates the JEM-X coded mask pattern.

III. Instrument operations

1. Telemetry formats and their use

A number of telemetry formats have been defined for the JEM-X instruments in order to make the best of a situation with a limited telemetry band-width. Two types of on-board data reduction can take place:

- 1) a grey filter can randomly remove *some of the events* from the telemetry data stream
- 2) a “reduced event” telemetry format removes *part of the information* about each event from the telemetry data stream. The telemetry format is selected by the user when preparing a proposal.

The so-called FULL IMAGING event data format is the standard format and is strongly recommended for almost all observation situations. The grey filter mechanism described in the next section works well to make the best use of the available telemetry capacity.

The FULL IMAGING format contains adequate information about event position, time, and energy. All the other formats remove part of that information from each event, thus requiring fewer bytes per event. A detailed description of the various formats is given in section 3 below. For each observation the observer must select a “primary” and a “secondary” format. When the observation starts the primary format (e.g. FULL IMAGING) will be in effect. If the actual count rate is too high for this format the instrument will autonomously switch to the secondary format. For JEM-X count rates higher than about 70 cts/s including background, or ~600 mCrab, the grey filter random event rejection will take place. Alternatively the user may specify a more densely packed “secondary” telemetry format at the cost of information per event. When the count rate exceeds a certain value the instrument will autonomously switch to this mode - and switch back when no longer needed. This, however, complicates the data analysis and experience shows that setting both the primary and the secondary format to FULL IMAGING is the best choice.

The conversion from recorded PHA value to energy depends on where the photons fall on the detector. Hence the non-imaging formats lead to a reduced energy resolution. The detector background is higher at the edge of the detector. The non-imaging formats include these edges that can be avoided in the imaging formats (FULL and RESTRICTED IMAGING). The RESTRICTED IMAGING mode, however, has very limited energy resolution.

The selection is made by the proposer when using the Proposal Generation Tool (PGT, see the “INTEGRAL Manual”).

2. The grey-filter mechanism

The grey-filter process can operate with 32 different transmission fractions. These fractions are $T = 1/32, 2/32, \dots, 31/32, 32/32$. The filter values to be used will be chosen by the instrument electronics during the actual observation, taking into account the total background count rates. The grey filter will always be adjusted automatically by the on-board software to match the data stream to the available telemetry capacity, thus the term “automatic grey filter”. Whenever the grey filter level is changed (decrease or increase) the on-board software checks whether a teleme-

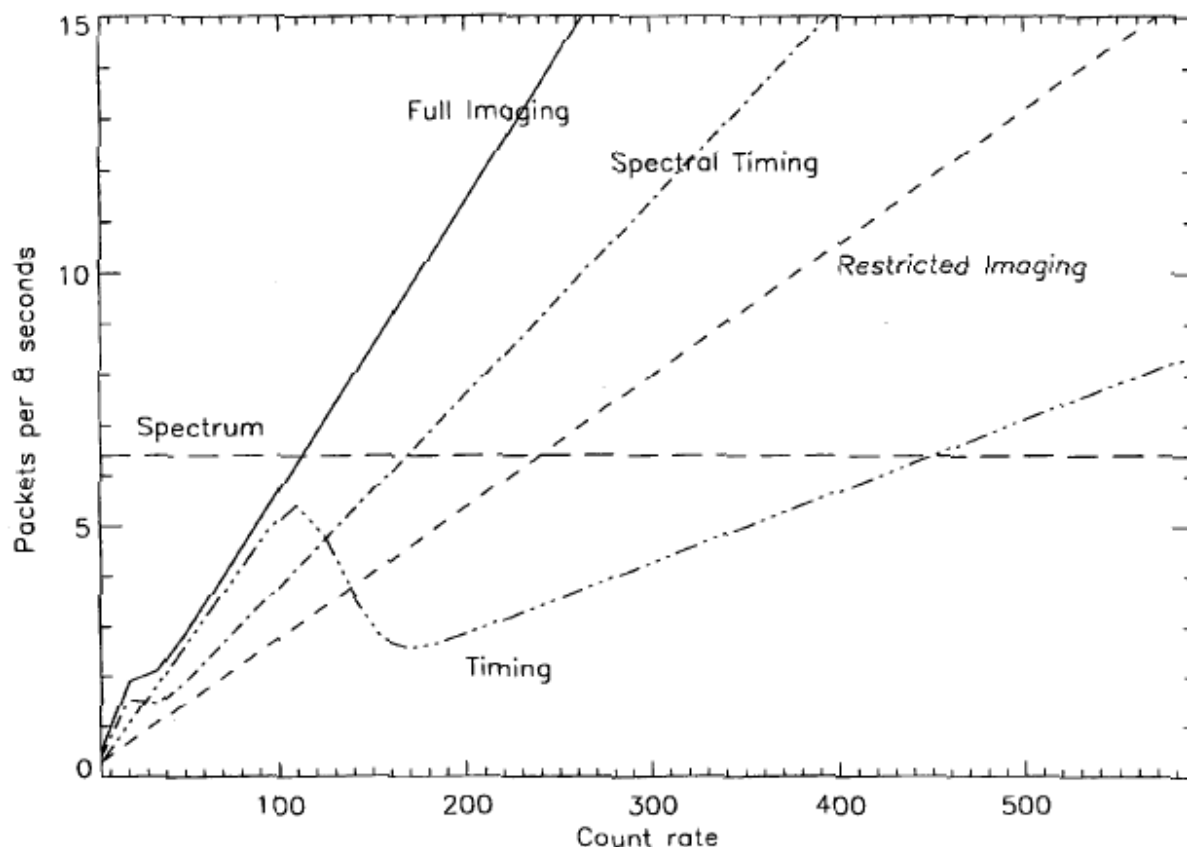


Figure 5. Telemetry rate per JEM-X unit, in packets per cycle of 8 seconds, for the 5 different telemetry modes: Full Imaging, Restricted Imaging, Spectral Timing, Timing and Spectrum. The maximum value for science data transmission, per JEM-X unit is $7/(8\text{ s})$

try format change should also take place. When the format changes from primary to secondary the value of the grey filter does not change initially. When the format switches back from secondary to primary the grey filter is automatically adjusted.

3. Detailed overview of the telemetry formats

The primary and secondary telemetry formats are the only instrumental parameters that need to be set by the general observer through the Proposal Generation software (PGT). Their characteristics are listed in Table 2. *We strongly recommend that for “normal” observations users select **FULL IMAGING** for both the primary and the secondary format* for it is the only way to ensure a good measurement of the X-ray background flux. (N.B. The rest of this section gives a detailed overview of the telemetry formats, so most observers can skip it and proceed to the next section).

Figure 5 shows the behavior of the telemetry rate versus count rate for the five JEM-X telemetry modes.

Table 2: Characteristics of the JEM-X Telemetry Formats

Format Name	Detector Image Resolution (pixels)	Timing Resolution	Number of Spectral Channels
Full Imaging	256 x 256	1/8192s = 122 μ s	256
Restricted Imaging	256 x 256	1/8 s = 125 ms	8
Spectral Timing	None	1/8192s = 122 μ s	256
Timing	None	1/8192s = 122 μ s	None
Spectrum	None	1/8s = 125 ms	64

Here are some further comments on the use of the telemetry formats (as primary or secondary):

FULL IMAGING: This is the main JEM-X format. It is recommended as primary and secondary format for most “standard” observations. If the count rate does not exceed 200 cts/s, no other formats should be considered. The event positions, pulse heights and arrival times are transmitted.

RESTRICTED IMAGING: This format should only be used as a secondary format (with FULL IMAGING as the primary format) and only in a situation where the purpose is to study a weak source close to a very strong source (> 2 Crab). This format provides all imaging capabilities of FULL IMAGING, but provides limited spectral resolution (8 channels) and timing resolution (1/8 s).

SPECTRAL TIMING: This format provides timing and spectral capabilities, but *no* imaging. It may be useful for observing fields with only one strong source, where imaging may be less important. It should be noted that actual physical spectral resolution is degraded because of the gain variation across the detector.

TIMING: Provides only the timing information of FULL IMAGING. The format is only suited for observations where one strong source dominates the field of view and where the interest is in the timing analysis. *No* position or spectral data is transmitted.

SPECTRUM: This format provides limited spectral resolution (64 channels) with limited time resolution (1/8 s). The format is only suited for observations where one strong source dominates the field of view. It is only to be considered at count rates above approximately 500 cts/s. *No* position data is transmitted.

3.1 Combining primary and secondary telemetry formats

When selecting the primary and the secondary format for a given observation only a restricted set of combinations is meaningful and possible. One essential rule is that the secondary format must not be less efficient in terms of event throughput than the primary format. Another constraint comes from the condition that the two formats to be combined as primary and secondary must have some significant data characteristics in common. For example, it does not make much sense to combine Restricted Imaging, which has only very limited timing and spectral capabilities, with the Spectral Timing, Timing or Spectrum formats. The Spectrum format does not combine with any of the other formats because the corresponding data are handled very differently on-board. These constraints are illustrated in Table 3. In case the same format is selected for primary and secondary, grey filtering will automatically switch in to limit the telemetry if the count rate limit is exceeded.

It should also be noted that, in the case of an amalgamation (see the “*Integral Manual*”, II 5.) of two or more observations, only the primary JEM-X telemetry format of the individual observations will come into consideration for JEM-X compatibility.

Table 3: Possible combinations of primary and secondary telemetry formats

Secondary Format→ Primary Format↓	Full Imaging	Restricted Imaging	Spectral Timing	Timing	Spectrum
Full Imaging	yes	yes	yes	yes	no
Restricted Imaging	no	yes	no	no	no
Spectral Timing	no	no	yes	yes	no
Timing	no	no	no	yes	no
Spectrum	no	no	no	no	yes

3.2 Ranges of usefulness of telemetry formats

Each telemetry format has a certain range of count rates which are optimal for the scientific priorities of an observation. Full Imaging is always optimal with respect to the amount of information about the transmitted events. However, only 70 events/s can be transmitted before the grey-filtering process will begin to reject good events (see Table 9 in section V for examples of real count rates). So, in very specific conditions, e.g. when observing crowded fields near the galactic centre or wanting to study a weak AGN in the vicinity of a bright source, the loss of events may not be acceptable and the Restricted Imaging format may be considered. In other cases, where the timing information is essential the Spectral Timing or pure Timing formats may be preferred despite the total loss of information about eventual background caused by other sources in the field. Table 4 shows the estimated ranges of usefulness of the different telemetry formats.

Table 4: Ranges of usefulness of telemetry formats

Format name	Rate of useful events (counts / second)	Preferred format with less restrictions
Full Imaging	70	None
Restricted Imaging	270	Full Imaging
Spectral Timing	180	Full Imaging
Timing	500	Spectral Timing
Spectrum	2000	Spectral Timing

IV. Performance of the instrument

JEM-X has now been tuned to stable operational conditions. Although these differ from what was originally planned before launch, the performance of JEM-X measured in orbit is close to pre-launch expectations.

1. Background

The JEM-X background in quiet solar conditions has been well measured for both units from a number of empty field observations. The background rate is about 20 counts/s in the 3 to 35 keV range, when the spacecraft is outside the radiation belts. This is about a factor 2 higher than predicted before launch. Figure 6 shows an empty field background spectrum taken by JEM-X in June 2004. The local radiation environment is mainly produced by two components: the diffuse X-ray background (DXB) and cosmic rays (CR). The diffuse X-ray background (DXB) dominates the background in the JEM-X energy range 3 -35 keV. The broad feature at about 30 keV is due to the injection of Xe fluorescence photons from the inactive gas volumes in the detector. (It is a good indicator of the effective resolution of the instrument). The contribution of secondary photons generated by primary cosmic rays is dominant above ~35 keV, outside the JEM-X energy range. The background increases noticeably at the edge of the detector. The rejection of background events produced by charged particles crossing the detector is accomplished with a combination of pulse height, pulse shape, anti-coincidence and “footprint” evaluation techniques. These techniques allow a particle rejection efficiency of >99.5%.

2. Timing stability and resolution

JEM-X observations of the Crab pulsar have shown that the timing is stable to better than 1 ns. However, the absolute timing is affected by an uncertainty of about 1 ms. The timing resolution of JEM-X is 122 micro-seconds, in the sense that each photon is determined to lie in a bin of that width. However, as the analysis shows, the phase of the timing bins is determined with a much better accuracy, consistent with the on-ground timing test results showing that the bin phase is accurate to a few micro-seconds.

3. Imaging: resolution and detection limits

The position determination accuracy depends on the number of source and background counts and on the position in the Field of View (FOV). The position is best determined for on-axis sources. Within the FCFOV (fully coded FOV) the collimator blocks some of the photons for sources in off-axis positions which also are affected by a weaker signal. In-orbit calibrations show

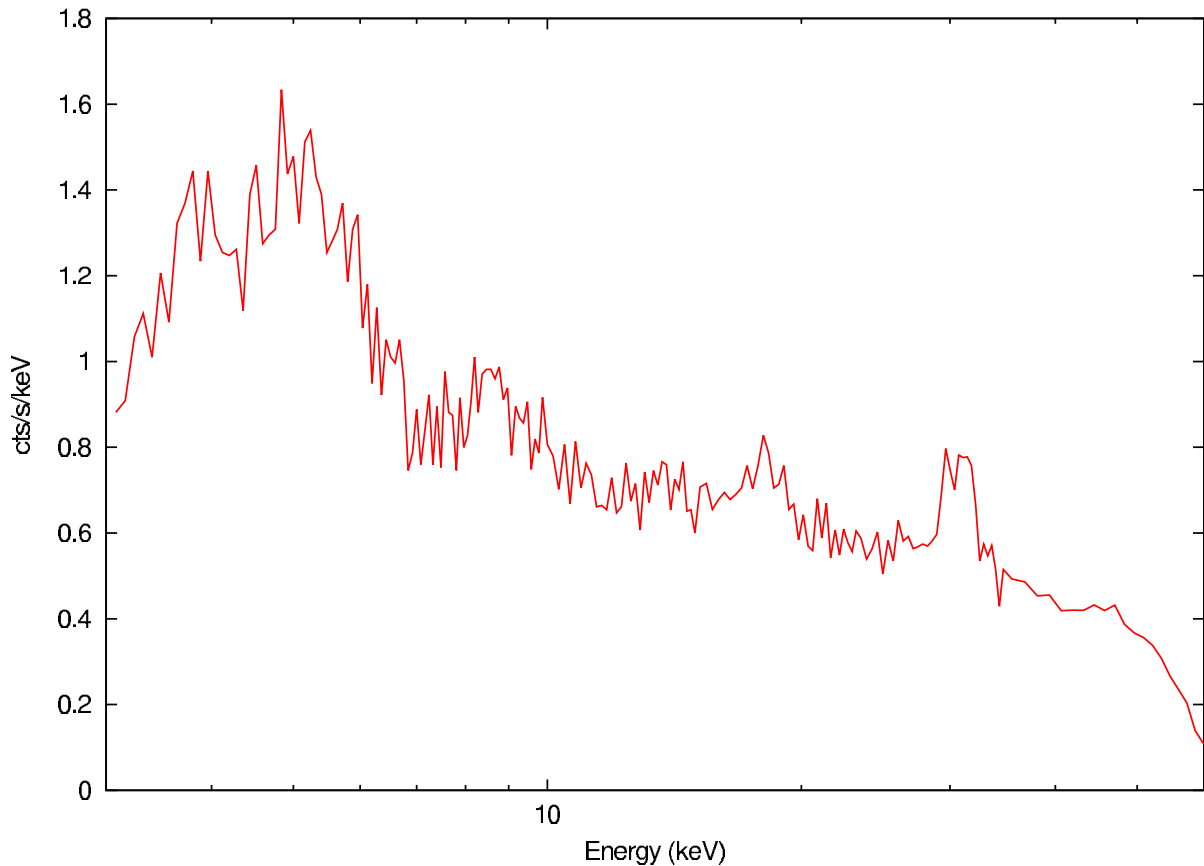


Figure 6. Empty field background spectrum observed on June 6, 2004 by the JEM-X 1 unit. The exposure time is 2200 s. The Xenon fluorescence line is clearly seen near 30 keV. At ~8 keV and ~20 keV there is a weaker Cu K-line and a Mo-K line

that the Point Spread Function of JEM-X is well represented by a symmetrical 2D Gaussian function with a standard deviation of 1.44 arcminutes. The position resolution as a function of energy is shown in Figure 7 for an on-axis source. The cause of the degradation below 10 keV is the signal-to-noise ratio of the front-end electronics. The energy dependence of the position resolution above 10 keV is determined by the increase of the primary photo-electron range with energy. The position resolution throughout the full energy range is finer than the pixel size of the coded mask.

Finally, there is an intrinsic systematic error on the position which also depends on the location within the field-of-view. For sources lying less than 4 degrees off axis the systematic errors are $<10''$. Between 4 and 5 degrees they appear to increase to about $20''$. Beyond 5 degrees we do not recommend to use JEM-X for source positioning. Indeed, at such off-axis distances the transmission of the collimator becomes very low.

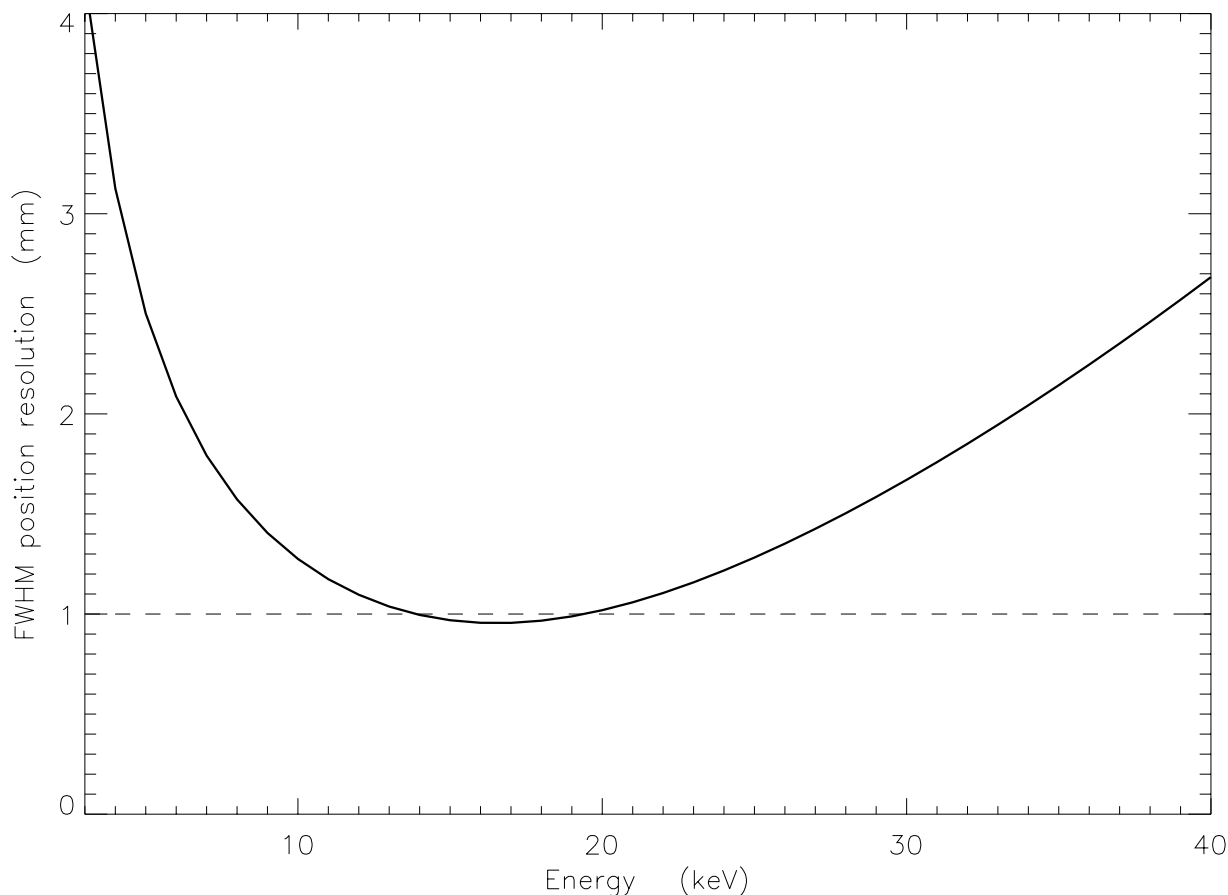


Figure 7. The position resolution in the detector as a function of energy. Note that the positions are rounded to 1mm accuracy in the down-linked data

4. Detector energy resolution

Laboratory tests show that the energy resolution of Micro Strip Gas Chambers degrades as a function of the detector gas pressure. The usual energy dependence of the resolution as function of energy, is obeyed at all investigated pressures:

$$\Delta E/E = C(E[\text{keV}])^{-1/2}$$

The proportionality factor C varies from 0.33 at 1 bar to 0.47 at 5 bar Xe/CH₄. Laboratory measurements with 90% Xe/10%CH₄ at 1.5 bar (the JEM-X values) show that the proportionality factor is C=0.4. Measurements in orbit have basically confirmed this result. However, it is now estab-

lished that the energy resolution of the JEM-X instruments degrade over time. This appears to be caused by gradual changes in the conductivity of the glass substrate due to ion migration. The JEM-X team will generate updates to the response files used at ISDC when needed in order to respond to this evolution.

The degradation of the energy resolution will be most noticeable at the highest energies. It can be described by an additional, slowly time-varying, term in the equation below:

$$\Delta E/E = 0.4 \times [(1/E[\text{keV}]) + (1/(E_{\text{noise}}[\text{keV}]))]^{1/2}$$

For JEM-X 1, at the present time, E_noise is close to 120 keV. As time passes this will decrease in magnitude corresponding to a progressively poorer energy resolution. For JEM-X 2 after 18 months of operation the E_noise value was about 15 keV. The JEM-X team is investigating ways of slowing the degradation rate.

5. Sensitivity (continuum and lines)

The JEM-X sensitivity measured in orbit is similar to the pre-launch predictions. Figure 8 shows the 3σ detection limit for a single JEM-X unit, as a function of observation time, using different assumptions about the FOV and imaging. Figure 9 shows the 3σ continuum sensitivity for a single JEM-X unit for different exposures.

Figures 10 and 11 show the detection limits for narrow lines at 6 keV (close to the Iron K line complex) and at 20 keV as well as the loci for 0.001, 0.1 and 1 keV Equivalent Width (EW).

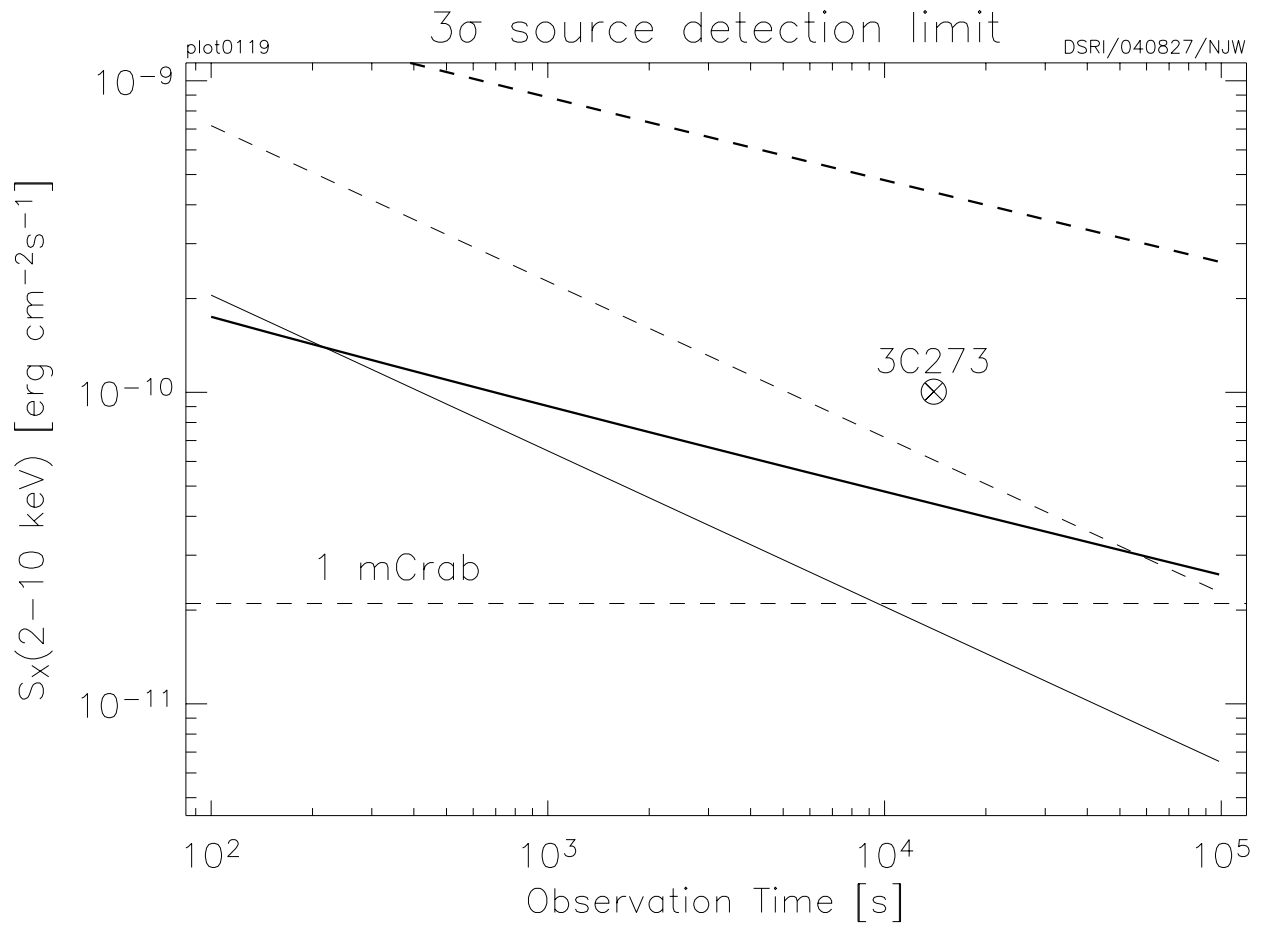


Figure 8. 3σ source detection limit as a function of exposure time for a single JEM-X unit when the source is on-axis. The lower thin solid curve has been calculated disregarding the imaging capability (using only the count rate). The thick solid curve represents the case when the source is being detected in the de-convolved image. In both cases no other sources are assumed to be present in the FOV. When there is a total of 1 Crab from extra sources then the dashed lines apply (lower dashed line: no imaging; upper dashed line: with imaging). The source strength is given in the interval 2 - 10 keV, but the 3 - 20 keV flux has been used for the detection limit. An actual 10σ detection by JEM-X of the source 3C 273 has been over-plotted. This is a 5 mCrab source and it was observed during 14000 s

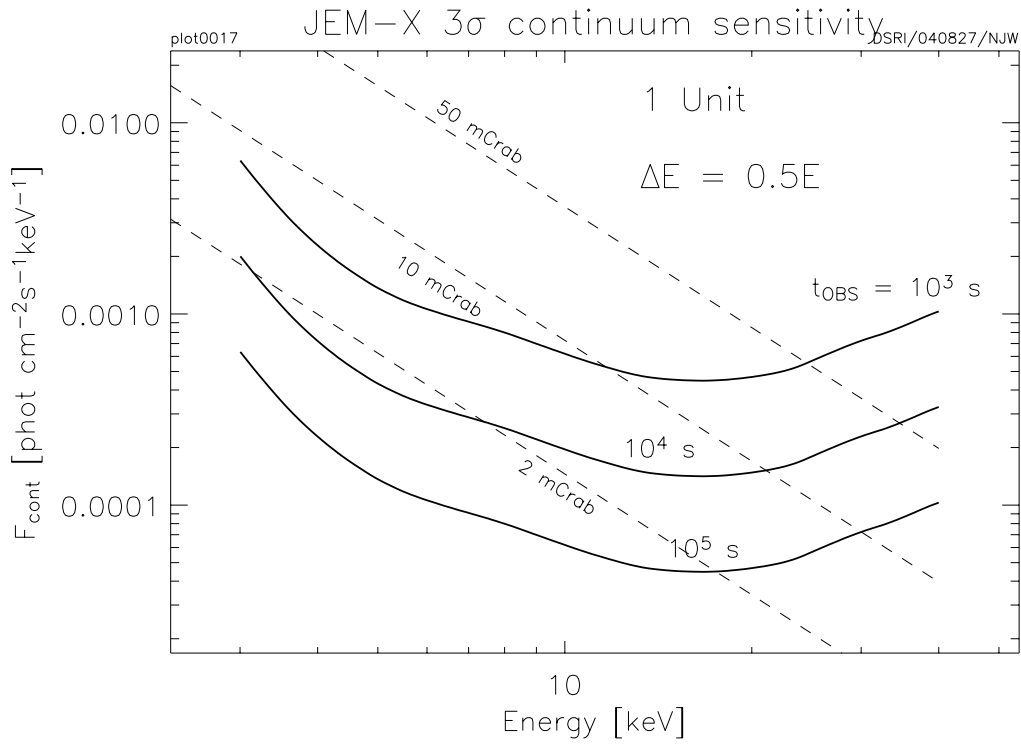


Figure 9. The 3σ continuum sensitivity for different exposure times. At each point on the curves the count rate and the background have been integrated over the energy bin in order to derive the detection limit. The dashed lines show Crab-like spectra for comparison

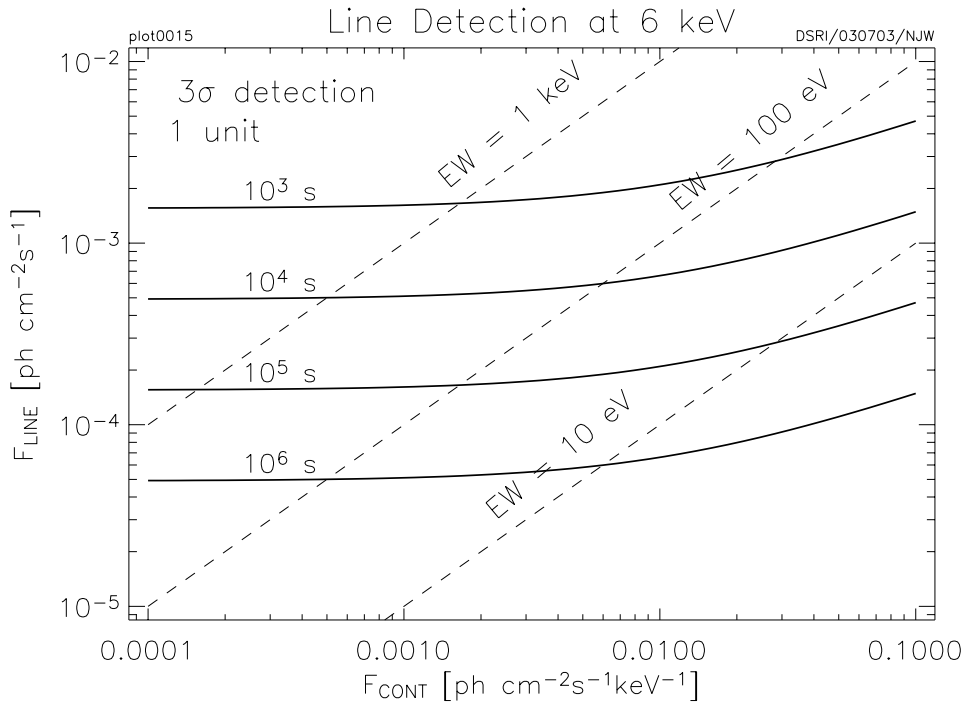


Figure 10 The 3σ line detection limits at 6 keV as a function of the continuum flux at 6 keV, for a single JEM-X unit. The dashed lines represent constant Equivalent Width (EW)

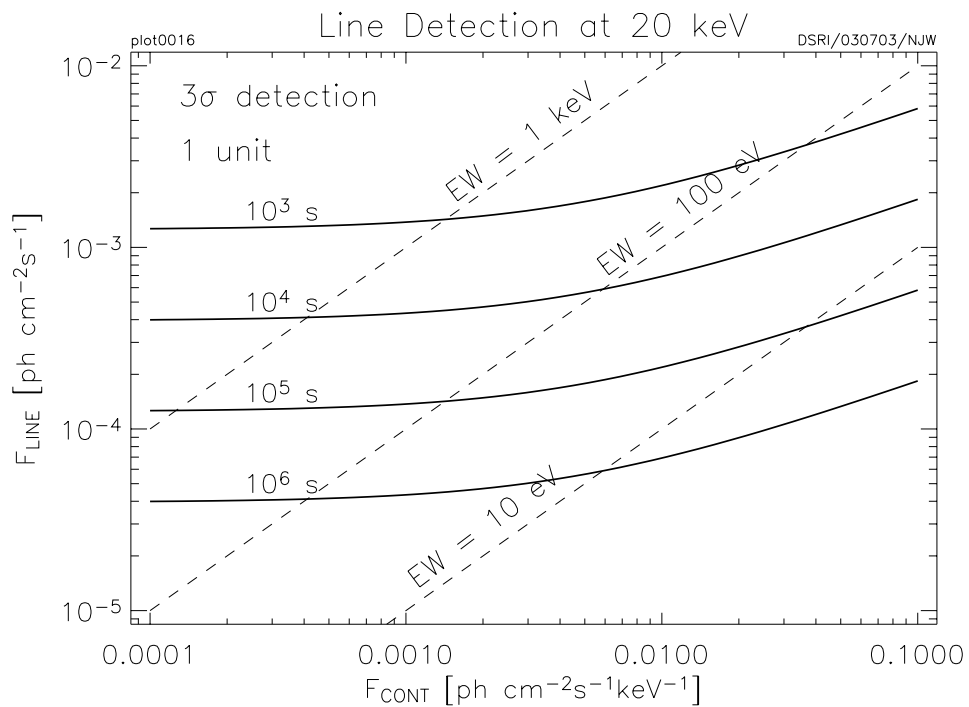


Figure 11. The 3σ line detection limits at 20 keV as a function of the continuum flux at 20 keV, for a single JEM-X unit. The dashed lines represent constant Equivalent Width (EW)

V. Observation “cook book”

1. Considerations of the use of the instrument

The primary role of JEM-X is to provide data on the X-ray flux and variability of the targets observed by the two main gamma-ray instruments IBIS and SPI. JEM-X can often pinpoint the source positions with a better precision than IBIS and is thus capable of contributing to the identification of new sources.

The sensitivity of a coded mask instrument like JEM-X is critically dependent on the software used to analyse the data - much more so than for simpler types of X-ray instruments. The sensitivity examples mentioned below should therefore not be considered as final - even after several months of intensive post-launch calibration work there are still several known shortcomings in the analysis software. Improvements in the spectrum extraction software are expected which may increase the S/N. Likewise, specific user choices during the data analysis can reduce the effective area to be used for a given JEM-X data set. This can lead to the necessity of using constant offsets when doing simultaneous spectral fitting of JEM-X spectra together with other Integral spectra.

Users should also be aware that the current spectral extraction and vignetting corrections for sources with off-axis angles greater than 3 or 4 degrees should be interpreted with caution.

Concerning the source detectability, it can be noted that during the Galactic Plane Scan observations (2200 s each) sources down to 20 mCrab are reliably detected when they are inside the central 10° of the field of view. In the same observations many weaker sources -down to 3 mCrab- are also found if they are within the central few degrees of the field of view. These numbers refer to observations with a single JEM-X unit.

2. Loss of JEM-X sensitivity due to dithering

Most INTEGRAL observations are done using a 5x5 dither pattern with points spaced 2° apart. Dithering is necessary for SPI and recommended for IBIS. Unfortunately, such dithering does not allow JEM-X to observe the target source continuously. In the 5x5 mode, only the central 9 out of the 25 dither pointings yield useful JEM-X spectral data for the central source. This is due to the fact that the target is off-axis during part of the dither pointings (see also Fig. 2). Table 5 shows the average degradation for the different spacecraft dithering patterns.

Table 5: Effective JEM-X observation times for different dithering modes

Dithering mode	Effective observation time
Staring	100%
Hexagonal dither	70%
“5 × 5” dither	34%

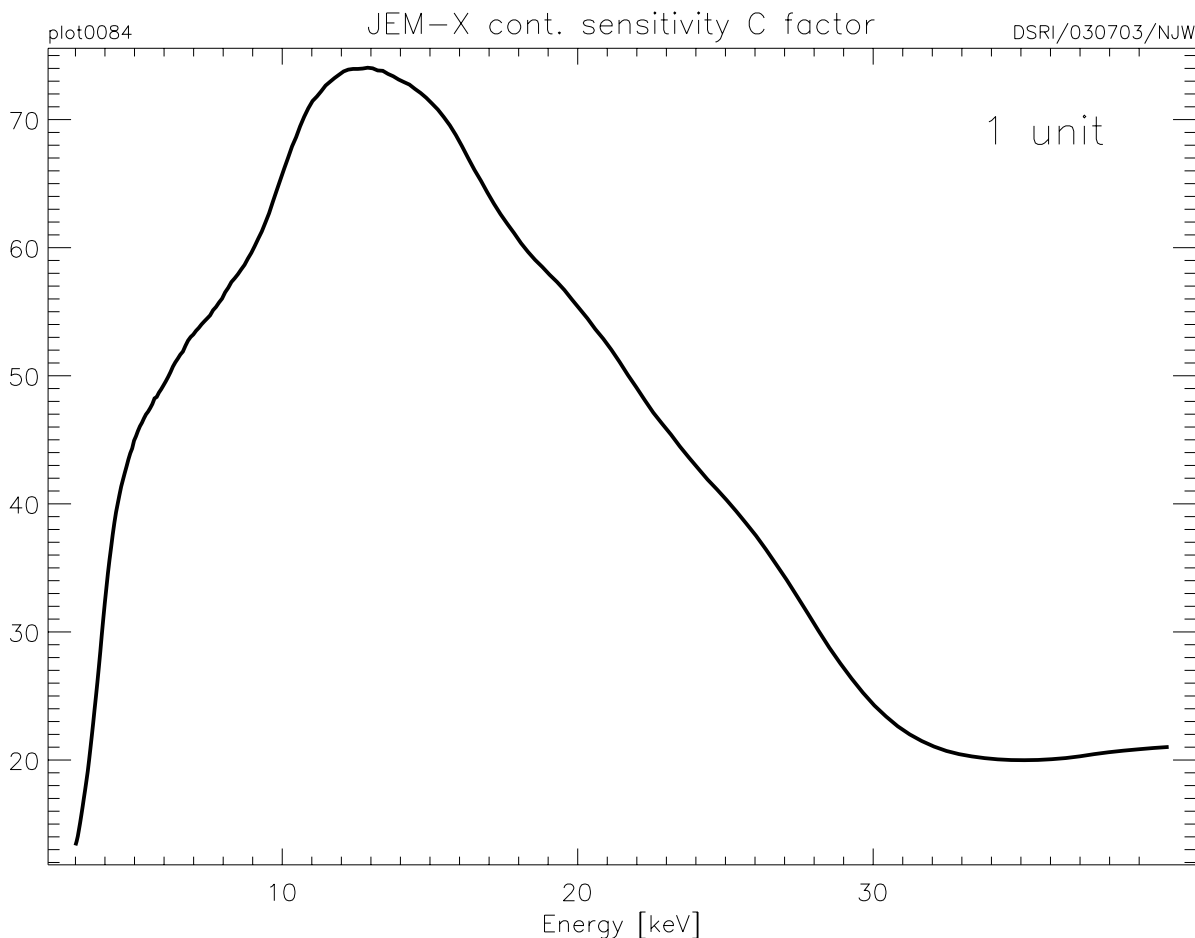


Figure 12. C-factor for estimating the continuum sensitivity, for a single JEM-X unit

3. How to estimate observing times

This section describes how to estimate observing times in order to detect X-ray continuum emission and line emission with JEM-X. It is assumed that there is *no dithering* (i.e. STARING mode) and that only *one* JEM-X unit is used. The instrument sensitivities quoted here are basically the same as in AO-2, however they are different from those described in AO-1. Observers may need to re-calculate their estimates accordingly!

3.1 Continuum emission

Figure 12 gives a plot of the factor $C(E)$ to be used together with the following equation in order to estimate the continuum sensitivity for various detection levels (N_σ = number of sigmas) and observation times t_{obs} (s). $F_{cont}(E)$ is the continuum flux (photons $\text{cm}^{-2} \text{s}^{-1} \text{keV}^{-1}$) and ΔE the energy resolution (keV):

$$N_\sigma = F_{cont}(E) \times \sqrt{(\Delta E \times t_{obs})} \times C(E)$$

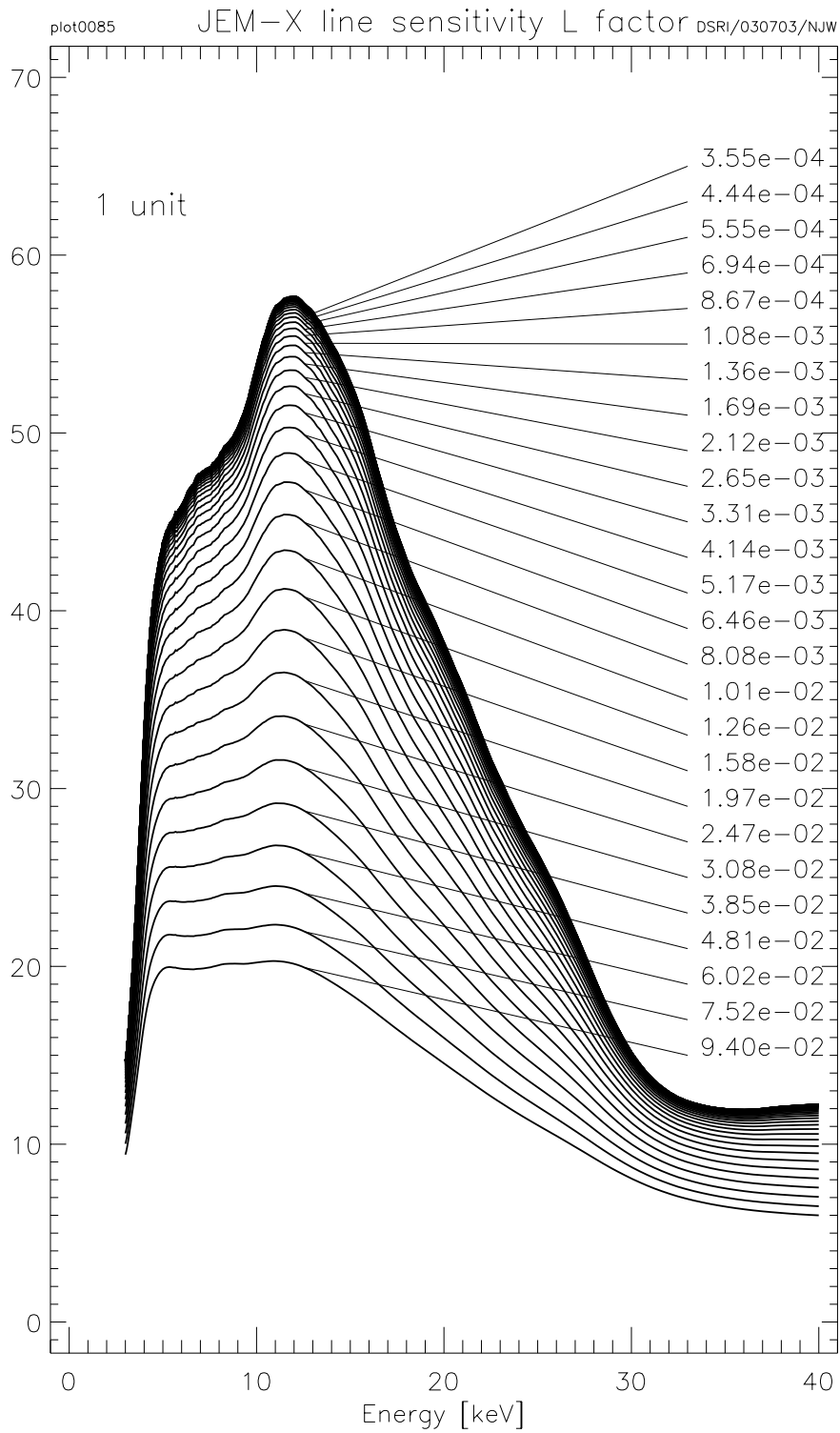


Figure 13. The L-factor for estimating the line detection sensitivity. There is a curve for each value of the continuum flux (indicated in photons $\text{cm}^{-2} \text{s}^{-1} \text{keV}^{-1}$). The L-factor is plotted as a function of the energy of the line feature and is for a single JEM-X unit

3.2 Line emission

Figure 13 gives a plot of the factor $L(E, F_{cont})$ to be used together with either of the following equations in order to estimate the line detection sensitivity for various detection levels (N_σ = number of sigmas) and observation times (t_{obs}).

$$N_\sigma = F_{line}(E) \times \sqrt{t_{obs}} \times L(E, F_{cont})$$

$$N_\sigma = F_{cont}(E) \times EW \times \sqrt{t_{obs}} \times L(E, F_{cont})$$

where $F_{line}(E)$ is the line flux (photons $\text{cm}^{-2} \text{s}^{-1}$), F_{cont} the source continuum flux at energy E (photons $\text{cm}^{-2} \text{s}^{-1} \text{keV}^{-1}$), and EW the equivalent width in keV.

4. Practical examples

This section gives some practical examples which illustrate the use the formulae described in section 2. To conclude, Table 9 lists the actual JEM-X background count rates for a single JEM-X unit as well as the observed count rates for the Crab (Nebula+pulsar) on-axis, as measured in-orbit.

4.1 Example #1: spectroscopy and continuum studies

Consider a 10 mCrab AGN with photon spectral index of 1.7. What is the capability of JEM-X for (i) spectroscopy, (ii) broad-band measurements?

Assume a staring observation, i.e. no sensitivity loss due to dithering.
Assume in each case that we want a 5σ measurement within a bandwidth ΔE .

For spectroscopy we choose a ΔE consistent with the spectral resolution at E : $\Delta E = 0.4 \times E^{1/2}$
It is clear from Table 6 that a short (10^5s) observation will not yield a high quality JEM-X spectrum on this source. However, for broad-band studies, choosing $\Delta E = E$, we at least achieve a measurement of the X-ray 'colour', as shown in Table 7.

Table 6: JEM-X spectroscopy

E(keV)	$\Delta E(\text{keV})$	Flux (photons $\text{cm}^{-2} \text{s}^{-1} \text{keV}^{-1}$)	C(E)	Required Observation Time (s)
4	0.8	5.0×10^{-4}	33	1.2×10^5
10	1.3	1.0×10^{-4}	67	4.3×10^5
20	1.8	3.0×10^{-5}	55	5.1×10^6

Table 7: JEM-X broad-band capability

E(keV)	ΔE (keV)	Flux (photons $\text{cm}^{-2}\text{s}^{-1}\text{keV}^{-1}$)	C(E)	Required Observation Time (s)
4	4	5.0×10^{-4}	33	2.3×10^4
10	10	1.0×10^{-4}	67	5.6×10^4
20	20	3.0×10^{-5}	55	4.6×10^5

4.2 Example #2: broad band variability

Consider a bright X-ray binary - 1/3 of the intensity of the Crab. We wish to perform a 'staring' observation of 9×10^4 s to measure the variability in two energy bands, 3-10 keV and 10-30 keV. How sensitive are we to rapid variability?

Table 8: N_σ for an exposure of 9×10^4 s

Band (keV)	E (keV)	ΔE (keV)	Flux (photons $\text{cm}^{-2}\text{s}^{-1}\text{keV}^{-1}$)	C(E)	N_σ in $t=9 \times 10^4$ s
3 - 10	6	7	0.09	50	3572
10 - 30	20	20	0.008	55	590

Assume we want a 5σ signal. The required time scales as the square of N_σ (see Table 8), so in the softer band we would achieve a 5σ signal in 0.2s, in the harder band in 6.5s.

4.3 Example #3: broad band variability and dithering

Consider the same source as in Example 2 but using a 5×5 dither pattern and performing the full scan just once, in 4.5×10^4 s. In addition, we have a 66% loss in sensitivity in this dither pattern compared to the staring observation in Example 2. The value of N_σ scales linearly with the sensitivity and as the square root of the integration time.

In this case (4.5×10^4 s) we achieve:

$$N_\sigma = 860 = (1-0.66) \times 0.09 \times (7 \times 4.5 \times 10^4)^{1/2} \times 50 \text{ at 6 keV and}$$

$$N_\sigma = 140 = (1-0.66) \times 0.008 \times (20 \times 4.5 \times 10^4)^{1/2} \times 55 \text{ at 20 keV.}$$

Times for a 5σ signal are 1.5 s and 57 s, respectively; however at every consecutive dither the effective sensitivity changes and this may introduce artifacts into the light curve on time-scales corresponding to the variable dither patterns.

4.4 Example #4: line detection

Consider a source with a power-law spectrum and spectral photon index = 1.5. It is expected to have a line feature at 20 keV with $EW = 0.5$ keV. The source strength in the interval 2 - 10 keV is 1.0×10^{-9} erg cm^{-2} s^{-1} .

$$F_{\text{cont}}(20 \text{ keV}) = 2.0 \cdot 10^{-3} \text{ photons } cm^{-2}s^{-1}keV^{-1},$$

$$F_{\text{line}} \text{ (expected)} = 1.0 \cdot 10^{-3} \text{ photons } cm^{-2}s^{-1},$$

$$L(E=20 \text{ keV}; F_{\text{cont}}=2.0 \cdot 10^{-3} \text{ photons } cm^{-2}s^{-1}keV^{-1}) = 36 \text{ (read from curve in Fig. 13),}$$

$t_{\text{obs}} = 4 \times 10^4$ s implies a detection level: $N_{\sigma} = 0.001 \times 200 \times 36 = 7.2$, which is a good detection.

4.5 Example #5: in-orbit count rates for the Crab and the JEM-X background

Table 9: Count rates for a single JEM-X unit (Crab on-axis)

Interval keV	Crab counts s^{-1}	DXB ^a counts s^{-1}	CR ^b induced counts s^{-1}	Total bkg counts s^{-1}
3 - 10	83	3	3.1	6.1
10 - 20	27	1.8	5.1	6.9
20 - 35	5.4	0.5	6.5	7.0
Total: 3 - 35	115	5.3	14.7	20.0

a. Diffuse X-ray background

b. Cosmic ray